~~New Strategy for~~ Focused Stark Deceleration

David Reens,* Hao Wu,† Alexander Aeppli, Anna McAuliffe, Piotr Wcisło, Tim Langen,‡ and Jun Ye
JILA, National Institute of Standards and Technology and the University of Colorado and Department of Physics, University of Colorado, Boulder, Colorado 80309-0440, USA
(Dated: January 22, 2020)

~~Since its first experimental realization, Stark deceleration has proven to be a useful tool for preparing molecular samples~~Stark deceleration is an important technology for cold and dense molecular beams, and has enabled numerous trapping and collisional studies. Nevertheless, Stark deceleration has ~~been prevented from realizing~~ not realized its full potential due to significant limitations in the ~~performance of the deceleration strategies thus far utilized~~focusing properties of Stark decelerators. We introduce a new ~~strategy that offers significant performance improvementsacross all useful operating conditions for a Stark decelerator. We demonstrate decelerator efficiency improvement by almost an order of magnitude through changing only the sequence of electric field switching without any modification to experimental setup. Additionally, we propose a strategy for further significant efficiency improvement that will require new high-voltage system. These techniques make~~ operation strategy that resolves focusing limitations but requires no hardware modifications. We explore the physics underlying these improvements, and verify our results for hydroxyl radicals. At trappable final velocities, molecule flux improves by a factor of 4.2 ± 0.8. The improvement factor is expected to scale inversely with the dipole moment to mass ratio, so that the application of Stark deceleration to ~~both~~ less readily polarized species ~~and longer devices~~ is now more feasible.

Over the past two decades, Stark deceleration has enabled groundbreaking collisional [1–3] and spectroscopic [4–7] studies of a variety of species [8]. Subsequent trap-loading greatly enhances interrogation time for such studies [9] and opens the door for further ~~cooling and manipulation [10, 11]~~manipulation [11]. Alongside the history of achievements enabled by Stark deceleration runs a parallel ongoing saga surrounding their efficient operation. Many important steps have been made, not only in understanding the flaws of the canonical pulsed decelerator [12, 13], but also in addressing them through the use of overtones [14, 15], undertones [16], or even mixed phase angles [17, 18]. Even with these advances, the outstanding inefficiencies of the pulsed decelerator, particularly with regard to transverse phase stability, have motivated alternative geometries such as interspersed quadrupole focusing [13] and traveling wave deceleration [19–21]. Although traveling wave deceleration takes a strong step ~~towards~~ toward truly efficient operation, it comes with significant engineering challenges. These may be partially addressed by the use of combination pulsed and traveling wave devices [22], or even using traveling wave geometry with pulsed electronics [23, 24]. In Zeeman deceleration, a parallel story ~~exists~~has unfolded, with early demonstrations [25, 26] later improved through the use of anti-Helmholtz configurations with better transverse focusing properties [27, 28]. Lacking a comparable breakthrough for Stark devices, others ~~continue~~ have continued to pursue brand new geometries [29], or even combine the best features of Stark and Zeeman approaches in a single device [30, 31]. Our strategy works with conventional geometry and electronics, but fully resolves transverse challenges and offers ~~more than fivefold~~ gains even at very low speeds.

The strategy is to admix new field distributions into the deceleration process that feature strong restoring ~~forces~~ force in the transverse directions. Depending on which field distributions are ~~chosen~~admixed, we specify several operating modes employing this strategy: focusing (F)~~and~~ , strong focusing (SF), and very strong focusing (VSF). In the conventional strategy~~(S = 1 and S = 3)~~, only two field distributions are used, and one is identical to the other up to translation. ~~SF mode mixes periods of transverse focusing within a conventional~~ Operation modes employing the conventional strategy (S = 1~~scheme using a 2D quadrupole field arrangement. F mode operates similarly, but utilizes multiple field configurations that time average to an effective 2D quadrupole potential as seen by the molecules in the slowed sample. Although this modeis weaker, it has the unique advantage of requiring no hardware modification to implement with an existing conventional decelerator.~~, S = 3) vary only in the timing of switches between these distributions. The measured performance of modes employing both strategies is shown in Fig. 1 for hydroxyl radicals, a benchmark species for Stark deceleration. These are performed on a decelerator not previously reported, with 2 mm pin spacing and other geometric parameters as in our earlier devices [32, 33], but with more than double the length, 333 stages, so as to decelerate a beam seeded in neon to rest. F mode, which requires no wiring changes and may be immediately employed on existing devices, enhances performance by a factor of $4 - 8$ depending on final speed, see Fig. 1. Modes SF and VSF are not implemented in this work, but could be achieved with a new high voltage system for additional significant enhancement factors according

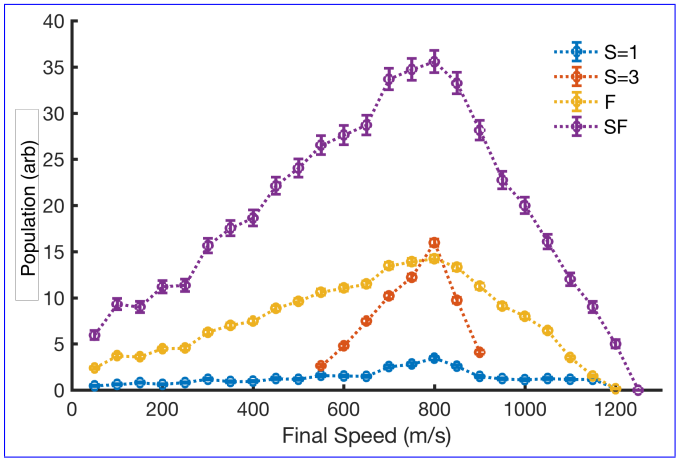

FIG. 1. ~~A new strategy for Stark deceleration, consisting~~ Experimental comparison of ~~altered timing sequences and transversely focusing electric field configurations~~deceleration strategies. ~~Left: On-axis energy diagrams for conventional operation modes S = 1 and new operation modes, strong focusing (SF) and focusing (F). Right: the field distributions utilized in these modes, A, B, and C/D, respectively. Prime indicates a spatial shift of the field configuration by one pin pair, e.g. A and A'. Distributions~~ Data are ~~generated in COMSOL~~ collected with ~~±12.5 kV applied; the chosen cut plane includes the~~ a 333 stage decelerator ~~axis~~ and ~~is 45° to all pins~~a beam of OH radicals expanded in Neon at an initial speed of 820 m/s. ~~In this plane~~Large gains persist at low speeds, ~~distributions B show clear focusing between grounded pin pairs~~with F, ~~and C/D work together to focus. Distribution A seems field free between grounded pins, but in~~ an operating mode employing the ~~plane orthogonal to the grounded pins it is in fact defocusing~~new strategy, ~~as evidenced by the traveling potential well generated by~~ outperforming S = 1 ~~mode in Fig~~at 25 m/s sixfold. ~~3b.~~

to our simulations, see Fig. 3.

To understand the success of this new strategy, we revisit the operating principle of a decelerator; Fig. 2 details field distributions and the operating modes derived from them. ~~It is customary to discuss the behavior of an idealized "synchronous molecule" sitting in the center of the slowed packet.~~ In the conventional ~~S = 1~~ strategy [8], ~~low-field seeking~~ molecules approach a charged pin pair, climbing a hill in potential energy (Fig. 2, ~~right~~ left column). The hill is abruptly switched off, allowing molecules to then repeat the process without regaining that potential energy. The ~~synchronous molecule loses an identical amount of energy at each pin pair. Since the~~ abrupt switch occurs partway up the potential energy hill, so that molecules that are ahead ~~of the synchronous molecule~~ get more energy removed, and vice versa. This creates a longitudinal restoring force for the molecules, with ~~the synchronous molecule existing at the effective trap center .~~

respect to the center of a decelerating reference frame. It is customary to imagine an idealized "synchronous molecule" sitting in the center of this frame. In the transverse directions, restoring force is not inherited from switching events, but arises directly from the focusing properties of field distributions in the lab frame. Together, the longitudinal and transverse restoring ~~forces~~ force generate a traveling potential well for the molecules, which translates along the device and decelerates according to ~~switching frequency ramp~~a programmed ramp of the switching frequency.

Conventionally, pins are always charged in bipolar pairs, in which case transverse focusing occurs right between the charged pin pair, but not significantly elsewhere (Fig. 2~~b-A). Indeed in the plane orthogonal to the grounded pin pair, the field is actually defocusing. Thus molecules~~ A). This causes molecules to experience much better transverse focusing when they are regularly sampling the focusing fields right between the charged pin-pair~~. This behavior is exploited in the use of deceleration overtones (S = 3, 5,) [14], where molecules are periodically allowed to transit between charged pin pairs. While this technique enhances focusing it sacrifices deceleration performance as fewer pins are used to slow. In the conventional S = 1 switching mode,~~ which requires them to be oscillating regularly ahead and behind the synchronous molecule. Just after the switching event, which as mentioned must happen only partway up the potential energy hill, molecules proceed through the largely field-free region between grounded pin pairs~~after a switching event~~. This region is of central importance to our new deceleration strategy. Useful field distributions with transverse focusing in this region can be created by applying voltage in a way that is not balanced between adjacent pin pairs. This imbalance causes field lines to run toward the grounded pin pair, creating a focusing 2D quadrupole structure, much like this one used intentionally for trapping and controlling spin-flip losses [11]. Imbalanced distributions include those arising from charging only a single rod (Fig. 2~~b-DE), or~~ DE), from charging a pin pair to the same voltage (Fig. 2~~b-B).~~ B), or from charging the other pin pair oppositely (Fig. 2C). These correspond to modes F~~and SF~~, SF, and VSF respectively. By implementing these distributions when the synchronous molecule is flying between the grounded pin pair, but retaining the use of the conventional distribution otherwise ~~,~~ (Fig. 2, upper–lower alignment), the longitudinal behavior of the device is preserved while the transverse behavior is vastly improved.

In order to quantitatively analyze these operation modes, we can directly calculate the traveling potential well ~~each sequence generates~~ they generate for the molecules. ~~Simulations are~~ This is performed as in [35, 36] but extended to three dimensions [37]. ~~We can inspect the efficiency improvements by calculating the total phase space remaining within the effective traveling well for a given deceleration and time, 3 ms as in the case of Fig. 3a. S = 1 demonstrates comparatively poor phase space preservation, only outperforming S = 3 and traveling wave(TW) systems at stronger decelerations~~

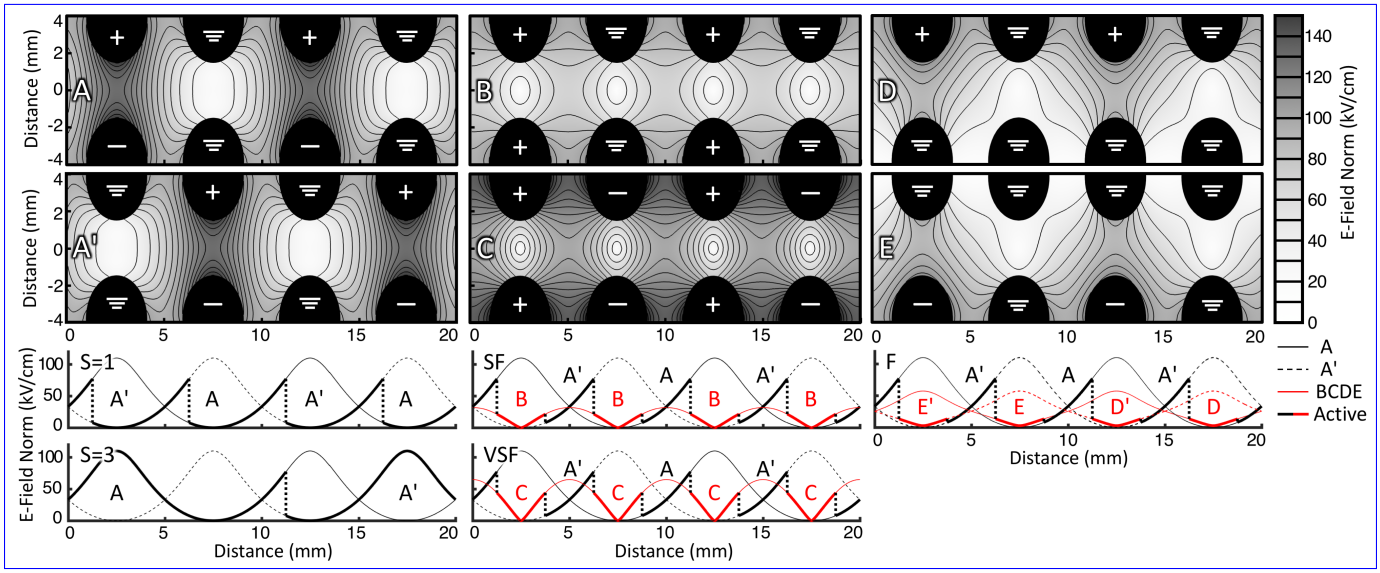

FIG. 2. A new strategy for Stark deceleration, consisting of novel distributions of the electric field and operation modes which employ them. Upper left: the conventional distribution (A) and its translation to the next pin pair (A'). Upper right: distributions featuring enhanced transverse focusing (B–E). Below: On-axis energy diagrams for conventional operation modes S = 1,3 [14]; and new operation modes named focusing (F), strong focusing (SF), and very strong focusing (VSF). These incorporate distributions D/E, B, and C respectively. Modes are aligned with the distributions they employ. Distributions are generated in COMSOL with ±12.5 kV applied; the chosen cut plane includes the decelerator axis and is 45° to all pins to ensure their visibility. In this plane, distributions B and C show clear focusing between grounded pin pairs, and D/E work together to focus. Distribution A seems field free between grounded pins, but in the plane orthogonal to the grounded pins it is in fact defocusing, as evidenced by the traveling potential well generated by S = 1 mode in Fig. 3.

~~where longitudinal loss is prohibitively high in these modes. Remarkably, F mode offers comparable phase space preservation to S = 3, but with no sacrifice in deceleration capability. SF mode makes more dramatic improvements, extending significant gains to even higher decelerations than possible with any other studied modes. For the traveling wave (TW) decelerator comparison in Fig. 3, 10 kV peak to peak sine waves are assumed, to our knowledge the largest used to decelerate all the way to rest [22]. Additionally, all modes besides TW use the rather small 2x2 mm^2 open area of our device, while TW devices use rings of 4 mm inner diameter. If the new modes were used with a 3×3 mm^2 [15] or a 4×4 mm^2 [38] device, phase space volume would increase significantly, depending approximately on the cube of pin-pair spacing.~~

The resulting wells may be visually inspected by plotting equipotential surfaces at various energies relative to the well minimum, see Fig. 3b. ~~Here we plot three dimensional potential energy surfaces for the three modes at three different energies for a deceleration of 200 km/s^2. The apparent holes in these surfaces occur when the surface reaches the 2×2 mm^2 transverse acceptance of our decelerator geometry. Molecules which reach this boundary~~ At some minimum escape energy E_{esc}, the traveling well equipotential fails to be closed, enabling molecules with energy $E \geq E_{esc}$ to escape. This escape may occur transversely, after which molecules encounter the surfaces of decelerator pins and are lost~~. Molecules may also be lost longitudinally, ceasing~~, or longitudinally, where molecules are not immediately lost but cease to remain in close proximity to the synchronous molecule. E_{esc} is plotted for all modes and as a function of varying decelerations in Fig. 3a. E_{esc} is a useful figure of merit for characterizing the performance of a given operating mode, as evidenced by the close agreement between Fig. 3a and Fig. 3c, where the volume of initial phase space which will remain in the traveling well after a 3 ms hold time is reported.

For the S = 1 mode, ~~the potential surface contains four small holes~~ E_{esc} is nearly zero, particularly for molecules which move away from the trap center towards the four small escape holes barely visible in the 10 mK S = 1 equipotential of Fig. 3b~~, illustrating that very low temperature molecules can still be lost if their trajectory intersects with one of these holes.~~. This is the underlying reason for the transverse-longitudinal coupling problem that has been described [12]. In general, such couplings are often useful for maintaining ergodicity in a potential well [39], but with some directions featuring very low escape energy, even small amounts of motional coupling lead to loss. ~~These loss regions actually reduce in size~~ E_{esc} actually improves with stronger deceleration for S = 1, as expected given the increased sampling of the transversely focusing region when molecules climb further towards the charged

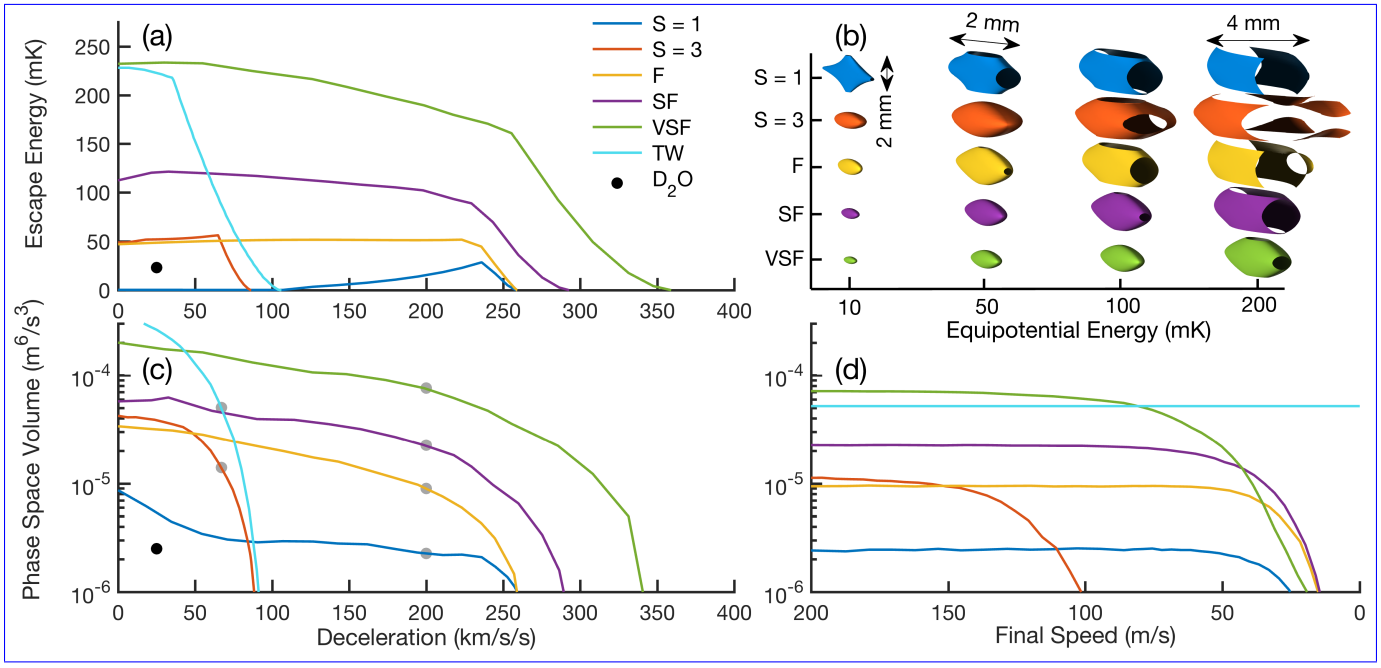

FIG. 3. ~~The traveling well simulation results of different deceleration modes. (a) Phase space volume~~ Escape energy E_{esc} from the traveling potential well generated by different modes of operation, for varying deceleration rate~~and an elapsed time of 3 ms~~. ~~A~~ Traveling wave (TW) deceleration is also compared, assuming a 10 kV peak to peak ~~traveling wave~~ waveform. (~~TW~~a) E_{esc} verse deceleration~~and ±12.5 kV S = 3 are also plotted~~. A point is shown for ~~comparison~~heavy water [34]. ~~Three solid dots correspond to the deceleration rate used in panel~~ (b) ~~and (c), respectively. (b)~~ Equipotentials of the traveling well for ~~three different~~ 200 km/s/s deceleration~~modes with deceleration rate 200 km/s^2~~, or 67 km/s/s for S = 3 since this mode requires a triple length device. Lack of closure of an equipotential ~~indicates the~~ equates to possibility of ~~molecule~~ escape. (c) ~~Phase Space Fillings~~Initial phase space volume remaining within the traveling well after 3 ms, ~~both longitudinal~~ only the effective traveling well is simulated. (~~top~~d) ~~and transverse~~ Full decelerator simulation, agreeing with (~~bottom~~c) at high enough final speeds, ~~for the labeled operation modes. Molecules travel 333 stages~~ studied with ~~an uniform initial distribution~~ varying final velocity but with hold time fixed at 3 ms and ~~an average speed of 900 m/s and a~~ deceleration ~~rate 200 km/s^2~~ fixed as indicated by the gray dots in panel (c). ~~The surviving number of molecules~~ For TW a full simulation is ~~3, 11 and 24 thousand respectively. Note dramatic improvements in homogeneity and flux, without signi?cant broadening~~ not performed; the value corresponding to ~~larger velocity classes~~the dot in panel (c) is shown for comparison.

pin pair~~. Through increased transverse confinement, F and SF modes significantly increase operation efficiency, demonstrating closed potential surfaces at~~ , see Fig. 2A. Remarkably, F mode offers comparable E_{esc} to S = 3, but with no sacrifice in deceleration capability. The SF and VSF modes make more dramatic improvements, with the latter rivaling traveling wave (TW) deceleration [19]. In Fig. 3, 10 ~~mK. Although F mode is clearly weaker than SF mode, both demonstrate a similar reduction in transverse-longitudinal coupling~~kV peak to peak sine waves are assumed, to our knowledge the largest used to decelerate all the way to rest [22]. Additionally, all modes besides TW use the rather small 2x2 mm^2 open area of our device, while TW devices use rings of 4 mm inner diameter. If VSF mode were used with a 3x3 mm^2 device [15] or a 4x4 mm^2 [38], phase space volume would increase significantly, depending approximately on the cube of pin-pair spacing.

The domain of validity of the use of traveling wells to characterize deceleration is a key concern. More commonly the traveling well approach is reserved for continuous deceleration schemes [19, 26]. Essentially it is required that the longitudinal velocity v_z of the molecules satisfy $v_z/D \gg f$, D the stage distance and f the oscillation frequency in the traveling well. The precise dynamics as one approaches this bound are relevant, especially for trapping experiments, which necessarily violate this condition as $v_z \to 0$. These dynamics may be precisely isolated by comparing the simulation of molecules in the traveling well (Fig. 3c) to full Monte-Carlo simulations. By varying only the final speed, and keeping deceleration and run-time exactly fixed by appropriately varying initial speed and decelerator length, we obtain the results shown in Fig. 3d. The asymptotically flat profiles at high enough speeds validate the traveling well approach, as do the quantitative agreement between the asymptotic values and the corresponding points at 200 km/s/s and 67 km/s/s in Fig. 3c.

The beginning of the low-speed breakdown depends on the intended use of the decelerator, and especially how far the molecules will be expected to travel unguided

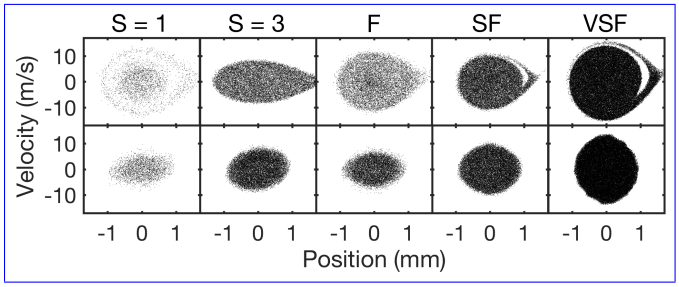

FIG. 4. Phase Space Fillings, both longitudinal (above) and transverse (below), for the labeled operation modes. With the same uniformly distributed initial phase space, the surviving number of molecules is 3, 17, 11, 24, and 75 thousand respectively. Note dramatic improvements in homogeneity and flux, without significant broadening to larger velocity classes except for VSF. Molecules travel 333 stages, begin at 900 m/s, and slow at 200 km/s/s (67 km/s/s for S = 3), large decelerations useful for trap loading.

afterwards. ~~For the range of decelerations and final speeds we used here the effective trap picture remains valid, see the appendix.~~ In Fig. 3c, the molecules still confined within a 3 mm diameter circle transversely after 5 mm free flight from the end of the sequence are shown. This is a conservative representation of what is required for trap-loading, but for collisional experiments a larger flight distance may be required. Note how F and SF cut off at even lower speeds than S = 1, but VSF cuts higher. This can be attributed to the fact that VSF actually features an increased transverse trap frequency relative to the others, while F and SF improve over S = 1 mostly by mitigation of escape minima, and not by increasing the transverse confinement strength of the well. VSF mode may be especially useful for trap loading in combination with a TW device as in [22].

In Fig. ~~3c~~4, the longitudinal and transverse phase space fillings are compared for all modes, with ~~200 km/s^2~~ 200 km/s/s deceleration through our 333 stage device, and final speeds of about 200 m/s to avoid low speed cut-off behavior. All modes are initialized with the same homogeneous phase space density (PSD). ~~The homogeneous initial phase space density used in Fig. 3c is valid when the initial beam source generates a much broader distribution in phase space than the volume accepted by the traveling potential well. In the longitudinal direction, most supersonic expansions satisfy this, with the exception of those performed with a Helium buffer gas, which can reach temperatures as low as 40 mK expanding from room temperature [40]. For this work, OH expands in neon and reaches a 300 mK longitudinal temperature [41], equivalent to a velocity spread of ±17 m/s. In the transverse direction, source temperature is a more subtle phenomenon, and may be bimodal [42] .~~ As can be seen, the distribution is nearly homogeneous after deceleration for all modes except S = 1. Increases in point density between panels do not arise from actual PSD increases, but from increases in the phase space volume that is projected onto the plane. Nevertheless, these improvements can prevent reductions in PSD which stem from under filling of the phase space volume that a trap can accept. For example, a hypothetical trap with an acceptance comparable to the outer dimensions of ~~the~~ S = 1 mode will be under filled by S = 1 deceleration due to the missing regions, while F mode will not do this, effectively quadrupling the phase space density loaded in the trap. Most realistic traps possess comparable transverse and longitudinal phase space acceptances due to ergodicity, cross-dimensional couplings, or cross-dimensionally thermalizing collisions if nothing else. In SF mode, transverse phase space acceptance is increased significantly over F mode, becoming comparable to the longitudinal, and avoiding transversely under filling ~~such~~ realistic traps by an additional factor of two.

~~The molecular signal and enhancement between F mode and conventional S=1 deceleration over a range of final speeds. Data are collected with a 333 stage decelerator with 25 kV between pins and a beam of OH radicals expanded in Neon at an initial speed of 825 m/s. Large gains persist at low speeds, with F outperforming S = 1 at 25 m/s by a factor of 7. The inset shows the time of flight signal from the valve pulse for F (orange) and S = 1(blue) modes measured at the end of the decelerator when slowing to 50 m/s, demonstrating a potential factor of 4 improvement at trappable final speeds.~~

The ~~measured enhancement of F over S = 1 is shown~~ homogeneous initial phase space density used in Fig. ~~1~~ for hydroxyl radicals, a benchmark species for Stark deceleration. ~~This is performed on a decelerator not previously reported, with 2 mm pin spacing and other geometric parameters as in our earlier devices [32, 33], but with more than double the length, 333 stages, so as to decelerate a beam seeded in neon with an initial speed of 825 m/s to rest. F mode, which may be immediately implemented on existing devices, enhances performance by at least a factor of 4, with an order of magnitude improvement at certain final speeds, see Fig. 1. Notably, F mode significantly improves operation at very low speeds (< 25 m/s), where S = 1 inefficiencies become readily apparent [9]. SF mode is not implemented in thiswork, but could be achieved with a new high voltage system for additional significant enhancement factors according to our simulations, see Fig. 3. Comparisons of decelerated populations between F mode and S = 1 mode at different applied voltages with a final velocity 50 m/s. The dot/square represent experimental results, which agree with the solid lines calculated from Monte Carlo simulation. Instead of showing saturation behavior as S = 1, the decelerated population using F mode increases with higher applied voltage.~~

~~An insightful way to experimentally understand this approach to transverse focusing is to operate using different confining potentials. Since our demonstration species the hydroxyl radical has a linear ground state~~

Stark shift in our standard operating field strengths, adjusting the voltage effectively linearly scale the potential experienced by the sample. Fig. ?? shows the final population of molecules slowed using S = 1 and F modes to 50 m/s, a typical trapping speed, under different decelerator voltages. Again, an equal amount of energy is removed from the synchronous molecule at each pin pair. At low voltages, the field between the pins is not sufficient to remove the energy required to slow to the desired speed. Past some point the field strength is sufficient to remove enough energy per stage such that the final speed can be achieved. Yet at higher voltages, molecules slowed in the S = 1 scheme do not need to approach the pins as closely, reducing the sampling of the inter-pin focusing field. Increased field gradients compete with a shorter focusing field sampling time. This behavior manifests as a saturation or even a reduction in the surviving molecule number, further discussed in [9]. Since the F mode separates transverse focusing from slowing, molecules experience greater transverse focusing at higher field strengths. Additionally, higher fields means that molecules need a shorter period of slowing and can spend a greater amount of time in the focussing field configuration. Thus at all but the lowest field strengths (where S = 1 is effectively equivalent to F mode) F mode slowing far outperforms the conventional deceleration strategy. While in this result we were limited to 13 kV by the safety margins of our device, one may be able to see considerable efficiency gains and greater phase space acceptances at even higher voltages using these advanced modes.

In addition to the two new operation modes identified here, a whole class of deceleration modes based upon the same strategy exists. Of significant interest is an enhanced transverse confinement mode we call very strong focusing(VSF). By charging the pin pairs in a +, − configuration instead of +, ground, as in SF, this mode effectively doubles the 2D quadrupole trap gradient, significantly enhancing transverse confinement. This technique utilizes two bipolar switches between ground and ±12 kV and two three state switches operating between all three voltage levels. There are other ways to achieve a similar result using different hardware configurations. 4 is valid when the initial beam source generates a much broader distribution in phase space than the volume accepted by the traveling potential well. In the longitudinal direction, most supersonic expansions satisfy this, with the exception of those performed with Helium buffer gas, which can reach temperatures as low as 40 mK expanding from room temperature [40]. For this work, OH expands in neon and reaches a 300 mK longitudinal temperature [41], equivalent to a velocity spread of ±17 m/s. In the transverse direction, source temperature is a more subtle phenomenon, and may be bimodal [42]. Furthermore, beam skimming and the resulting interference it causes often requires require increased distance between the source and the decelerator, resulting in a transversely under-filled traveling well. Skimmer cooling addresses this [41], and is therefore well suited for VSF mode.

Finally, we note that the enhanced applicability of deceleration to less responsive molecules. D_2O molecules in the $|1,1\rangle$ state [34] are brought into the viable range in VSF mode, note the point at 25 km/s/s in Fig. 3c. This is discussed further here [37].

We introduce a new deceleration strategy, with several accompanying modes of operation for the conventional pulsed decelerator. Significant improvements in transverse focusing and overall performance are demonstrated. The strategy does not simply increase the temperature of molecules which may be decelerated. Instead, by introducing periods of separate transverse focusingincreasing the minimum escape energy E_{esc} from the traveling potential well, molecule flux is enhanced at the same temperatures as before. This discovery opens up possibilities for applying Stark deceleration to faster beams or to molecules with less favorable Stark shift to mass ratiosratio, since decelerator length may be extended without suffering from low temperature molecule loss E_{esc} in the traveling well.

* dave.reens@colorado.edu.; Present Address: Lincoln Laboratory, Massachusetts Institute of Technology, Lexington, Massachusetts 02420, USA
† Present Address: Department of Physics and Astronomy, University of California, Los Angeles, California 90095, USA
‡ Present Address: 5. Physikalisches Institut and Center for Integrated Quantum Science and Technology (IQST), Universität Stuttgart, Pfaffenwaldring 57, 70569 Stuttgart, Germany

[1] B. C. Sawyer, B. K. Stuhl, M. Yeo, T. V. Tscherbul, M. T. Hummon, Y. Xia, J. Kłos, D. Patterson, J. M. Doyle, and J. Ye, Physical Chemistry Chemical Physics **13**, 19059 (2011).
[2] M. Kirste, X. Wang, H. C. Schewe, G. Meijer, K. Liu, A. van der Avoird, L. M. C. Janssen, K. B. Gubbels, G. C. Groenenboom, and S. Y. T. van de Meerakker, Science **338**, 1060 (2012).
[3] Z. Gao, T. Karman, S. N. Vogels, M. Besemer, A. van der Avoird, G. C. Groenenboom, and S. Y. T. van de Meerakker, Nature Chemistry **10**, 469 (2018).
[4] J. Veldhoven, J. K upper, H. L. Bethlem, B. Sartakov, A. J. A. Roij, and G. Meijer, The European Physical Journal D **31**, 337 (2004).
[5] E. R. Hudson, H. J. Lewandowski, B. C. Sawyer, and J. Ye, Physical Review Letters **96**, 143004 (2006).
[6] B. L. Lev, E. R. Meyer, E. R. Hudson, B. C. Sawyer, J. L. Bohn, and J. Ye, Physical Review A **74**, 061402 (2006).
[7] A. Fast, J. E. Furneaux, and S. A. Meek, Physical Review A **98**, 052511 (2018).
[8] S. Y. T. van de Meerakker, H. L. Bethlem, N. Vanhaecke,

and G. Meijer, Chemical Reviews **112**, 4828 (2012).
[9] B. C. Sawyer, B. K. Stuhl, D. Wang, M. Yeo, and J. Ye, Physical Review Letters **101**, 203203 (2008).
[10] B. K. Stuhl, M. T. Hummon, M. Yeo, G. Quéméner, J. L. Bohn, and J. Ye, Nature **492**, 396 (2012).
[11] D. Reens, H. Wu, T. Langen, and J. Ye, Physical Review A **96**, 063420 (2017).
[12] S. Y. T. van de Meerakker, N. Vanhaecke, and G. Meijer, Annual Review of Physical Chemistry **57**, 159 (2006).
[13] B. C. Sawyer, B. K. Stuhl, B. L. Lev, J. Ye, and E. R. Hudson, European Physical Journal D **48**, 197 (2008).
[14] S. Y. T. van de Meerakker, N. Vanhaecke, H. L. Bethlem, and G. Meijer, Physical Review A **71**, 053409 (2005).
[15] L. Scharfenberg, H. Haak, G. Meijer, and S. Y. T. van de Meerakker, Physical Review A **79**, 023410 (2009).
[16] D. Zhang, G. Meijer, and N. Vanhaecke, Physical Review A **93**, 023408 (2016).
[17] L. P. Parazzoli, N. Fitch, D. S. Lobser, and H. J. Lewandowski, New Journal of Physics **11**, 055031 (2009).
[18] S. Hou, S. Li, L. Deng, and J. Yin, Journal of Physics B: Atomic, Molecular and Optical Physics **46**, 045301 (2013).
[19] A. Osterwalder, S. A. Meek, G. Hammer, H. Haak, and G. Meijer, Physical Review A **81**, 051401 (2010).
[20] J. van den Berg, S. Mathavan, C. Meinema, J. Nauta, T. Nijbroek, K. Jungmann, H. Bethlem, and S. Hoekstra, Journal of Molecular Spectroscopy **300**, 22 (2014).
[21] M. I. Fabrikant, T. Li, N. J. Fitch, N. Farrow, J. D. Weinstein, and H. J. Lewandowski, Physical Review A **90**, 033418 (2014).
[22] M. Quintero-Pérez, P. Jansen, T. E. Wall, J. E. van den Berg, S. Hoekstra, and H. L. Bethlem, Physical Review Letters **110**, 133003 (2013).
[23] S. Hou, Q. Wang, L. Deng, and J. Yin, Journal of Physics B: Atomic, Molecular and Optical Physics **49**, 065301 (2016).
[24] Y. Shyur, J. A. Bossert, and H. J. Lewandowski, Journal of Physics B: Atomic, Molecular and Optical Physics **51**, 165101 (2018).
[25] N. Vanhaecke, U. Meier, M. Andrist, B. H. Meier, and F. Merkt, Phys. Rev. A **75**, 31402 (2007).
[26] E. Narevicius, A. Libson, C. G. Parthey, I. Chavez, J. Narevicius, U. Even, and M. G. Raizen, Physical Review Letters **100**, 093003 (2008).
[27] E. Lavert-Ofir, S. Gersten, A. B. Henson, I. Shani, L. David, J. Narevicius, and E. Narevicius, New Journal of Physics **13**, 103030 (2011).
[28] K. Dulitz, M. Motsch, N. Vanhaecke, and T. P. Softley, The Journal of Chemical Physics **140**, 104201 (2014).
[29] Q. Wang, S. Hou, L. Xu, and J. Yin, Physical Chemistry Chemical Physics **18**, 5432 (2016).
[30] T. Cremers, S. Chefdeville, N. Janssen, E. Sweers, S. Koot, P. Claus, and S. Y. T. van de Meerakker, Phys. Rev. A **95**, 43415 (2017).
[31] V. Plomp, Z. Gao, T. Cremers, and S. Y. T. van de Meerakker, Physical Review A **99**, 33417 (2019).
[32] J. R. Bochinski, E. R. Hudson, H. J. Lewandowski, and J. Ye, Physical Review A **70**, 043410 (2004).
[33] B. C. Sawyer, B. L. Lev, E. R. Hudson, B. K. Stuhl, M. Lara, J. L. Bohn, and J. Ye, Physical Review Letters **98**, 253002 (2007).
[34] M. Motsch, L. D. van Buuren, C. Sommer, M. Zeppenfeld, G. Rempe, and P. W. H. Pinkse, Physical Review A **79**, 013405 (2009).
[35] H. L. Bethlem, G. Berden, A. J. A. van Roij, F. M. H. Crompvoets, and G. Meijer, Physical Review Letters **84**, 5744 (2000).
[36] E. R. Hudson, J. R. Bochinski, H. J. Lewandowski, B. C. Sawyer, and J. Ye, The European Physical Journal D **31**, 351 (2004).
[37] See Supplementary Materials.
[38] S. Y. T. van de Meerakker, P. H. M. Smeets, N. Vanhaecke, R. T. Jongma, and G. Meijer, Physical Review Letters **94**, 023004 (2005).
[39] E. L. Surkov, J. T. M. Walraven, and G. V. Shlyapnikov, Physical Review A **53**, 3403 (1996).
[40] U. Even, Advances in Chemistry **2014**, 636042 (2014).
[41] H. Wu, D. Reens, T. Langen, Y. Shagam, D. Fontecha, and J. Ye, Physical Chemistry Chemical Physics **20**, 11615 (2018).
[42] H. Beijerinck and N. Verster, Physica B+C **111**, 327 (1981).